Quantum confinement effect in thin quantum wires

Jian-Bai Xia* and K. W. Cheah†
Department of Physics, Hong Kong Baptist University, Kowloon Tong, Hong Kong
(Received 3 June 1996; revised manuscript received 17 March 1997)

The electronic states and optical transition properties of three semiconductor wires Si, GaAs, and ZnSe are studied by the empirical pseudopotential homojunction model. The energy levels, wave functions, optical transition matrix elements, and lifetimes are obtained for wires of square cross section with width from 2 to 5 $(\sqrt{2}a/2)$, where a is the lattice constant. It is found that these three kinds of wires have different quantum confinement properties. For Si wires, the energy gap is pseudodirect, and the wave function of the electronic ground state consists mainly of four bulk Δ states. The optical transition matrix elements are much smaller than that of a direct transition, and increase with decreasing wire width. Where the width of wire is 7.7 Å, the Si wire changes from an indirect energy gap to a direct energy gap due to mixing of the bulk Γ_{15} state. For GaAs wires, the energy gap is also pseudodirect in the width range considered, but the optical transition matrix elements are larger than those of Si wires by two orders of magnitude for the same width. However, there is no transfer to a direct energy gap as the wire width decreases. For ZnSe wires, the energy gap is always direct, and the optical transition matrix elements are comparable to those of the direct energy gap bulk semiconductors. They decrease with decreasing wire width due to mixing of the bulk Γ_1 state with other states. All quantum confinement properties are discussed and explained by our theoretical model and the semiconductor energy band structures derived. The calculated lifetimes of the Si wire, and the positions of photoluminescence peaks, are in good agreement with experimental results. [S0163-1829(97)08424-5]

I. INTRODUCTION

Recent experiments on porous Si have demonstrated efficient room-temperature visible photoluminescence (PL).[1] The etching process produces material consisting mainly of columns or wires with widths ≤50 Å of crystalline Si.[2] The nature of the luminescence process is currently the subject of numerous experimental and theoretical studies. There have been several mechanisms proposed, namely, the quantum confinement effect,[1,2] specific molecular agents such as siloxene,[3,4] surface-related states,[5,6] etc. For the quantum confinement effect there have been many theoretical works.[7–10] Most of the theoretical works, including tight-binding calculations,[7] empirical pseudopotential calculations,[8,9] and first-principles pseudopotential calculations,[10–12] have shown that quantum confinement increases the minimum band-gap energy and leads to a pseudodirect gap at the center of the Brillouin zone. The conduction-band-minimum wave functions retain a large composition from near the Δ minimum of the bulk Si conduction band. Experimental observations of the phonon-related fine structure in low-temperature PL,[13] the combined photoluminescence and absorption studies,[14] and the model calculations point to optical transition with weak oscillator strength, with phonon-assisted transition dominant for red emission. The room-temperature time-resolved PL experiments found two different emission bands:[13] the low-energy S band and the high-energy F band. The low-energy S band peaks in the deep red (1.72 eV) and with an overall room-temperature lifetime of $\sim 3\times10^{-5}$ s. Its integrated intensity accounts for 97% of the red emission from conventional porous silicon. Examining the lifetimes at different emission energies shows that these could be fitted by assuming two decay channels with an energy difference in the range of 10–30 meV. The upper level lifetime is around 5 μs ("slow"), and the lifetime of the lower level is around 3 ms ("very slow"). The high-energy F-band peaks at the green-blue (2.4 eV), and a decay time is faster than 3×10^{-8} s. This accounts for only 1–3 % of the emission in conventional porous silicon.

In this paper we use the empirical pseudopotential homojunction model[8] to calculate the electronic states and corresponding lifetimes of optical transition for Si thin quantum wires. The results verify the two decay channels model proposed by Calcott *et al.*,[13] and verify further that there exist optical transitions caused by quantum confinement states in the porous silicon, though it is not the main mechanism for the strong luminescence. For comparison we also calculate the electronic states and corresponding lifetimes for GaAs and ZnSe quantum wires. GaAs and ZnSe are III-V and II-VI semiconductor compounds, respectively, and they are all direct-gap semiconductors. The calculation found that the electronic state properties are extremely different for these two thin quantum wires; the GaAs wire becomes an indirect energy gap semiconductor just as the Si wire, while the ZnSe wire is still a direct energy gap semiconductor. The reason is shown by our model. Section II gives the theoretical model. Sections III and IV are the results for the Si and GaAs and ZnSe thin quantum wires, respectively. Section V contains a summary.

II. EMPIRICAL PSEUDOPOTENTIAL HOMOJUNCTION MODEL (REF. 8)

We use the supercell model to study a free-standing wire with a square cross section, as shown in Fig. 1. The system has translational symmetries in the [110], $[\bar{1}10]$, and [001] directions with periods $(l\sqrt{2}/2)a$, $(\sqrt{2}/2)a$, and a, where

0163-1829/97/55(23)/15688(6)/$10.00 © 1997 The American Physical Society

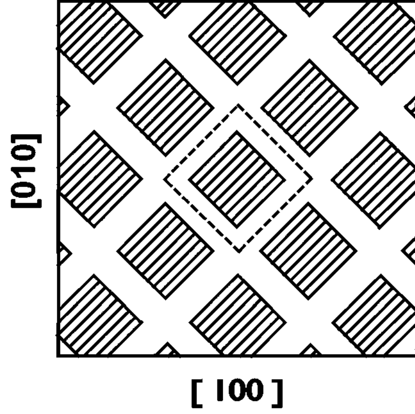

FIG. 1. Schematic plot of the cross section of square standing wires. The filled area is the wire region, the open area is the vacuum region. The dashed line signs the super unit cell in the x-y plane.

l is an integer which determines the size of the unit cell, and a is the lattice constant. Because of the periodicity of the system, the wave function of the wire can be written in terms of its bulk states with wave vectors $\mathbf{k}+\mathbf{g}$, where $\mathbf{g}$ are reciprocal-lattice vectors of the model system enclosed within the first Brillouin zone of the bulk material. Here we use a double unit cell with the basic vectors

$$\mathbf{a}_1=\frac{a}{2}(1,1,0),\quad \mathbf{a}_2=\frac{a}{2}(-1,1,0),\quad \mathbf{a}_3=a(0,0,1),\quad (1)$$

instead of the usual unit cell of the diamond structure, in order to satisfy the periodicity. The components of $\mathbf{g}$ along the $[110]$ and $[\bar{1}10]$ directions are given by

$$g_1=\frac{2\pi}{l\frac{\sqrt{2}}{2}a}l_1,$$

$$l_1=-[(l-1)/2],\ldots,0,\ldots,[l/2], \quad (2)$$

$$g_2=\frac{2\pi}{l\frac{\sqrt{2}}{2}a}l_2, \quad (3)$$

$$l_2=-[(l-1)/2],\ldots,0,\ldots,[1/2], \quad (4)$$

where we used the symbol $[x]$ to denote an integer closest to and no larger than x. Using these bulk states as basis functions for the expansion of the wave functions of wire, we have

$$\Psi(\mathbf{r})=\sum_{n,\mathbf{g}} C_{n,\mathbf{k}+\mathbf{g}}\psi_{n,\mathbf{k}+\mathbf{g}}(\mathbf{r}), \quad (5)$$

where $\psi_{n,\mathbf{k}+\mathbf{g}}$ represents the bulk Bloch states associated with the n-th band and wave vector $\mathbf{k}+\mathbf{g}$,

We assume that the perturbation potential in the vacuum region (the open area in Fig. 1) $\Delta V(\mathbf{r})=V_0$, while in the wire region (the filled area in Fig. 1) $\Delta V(\mathbf{r})=0$, where V_0 is large relative to the energy range considered. It is positive for the conduction-band states and negative for the valence-band states. That is, the vacuum regions are replaced by the same bulk material with the conduction bands rigidly shifted upward by a constant and the valence bands shifted downward by another constant. The problem now resembles that of a homojunction. The mixing of conduction and valence-band states is neglected by solving the problem separately for conduction and valence bands. That means that first we project all the plane waves on to the bulk conduction-band subspace and the bulk valence-band subspace, then we calculate the electron and hole states of the wire in these two subspaces, respectively. This is a reasonable approximation because the energy gap between the electron and hole states increases with the quantum confinement strengthening, and the mixing of conduction and valence-band states becomes smaller and smaller.

Using the degenerate perturbation theory, we obtain a secular equation for the wire,

$$|E_{n,\mathbf{k}+\mathbf{g}}\delta_{nn'}\delta_{\mathbf{g}\mathbf{g}'}+\langle n,\mathbf{k}+\mathbf{g}|\Delta V|n',\mathbf{k}+\mathbf{g}'\rangle-E|=0, \quad (6)$$

where $E_{n,\mathbf{k}}$ is the energy eigenvalues of the bulk. In the coordinate system with the x and y axes along the $[110]$ and $[\bar{1}10]$ directions, respectively, the matrix elements of the perturbation potential can be written as

$$\langle\mathbf{g}+\mathbf{G}|\Delta V|\mathbf{g}'+\mathbf{G}'\rangle=V_0\frac{l^2-m^2}{l^2}\quad \text{for } \Delta G_x=0,\ \Delta G_y=0,$$

$$-V_0\frac{2m}{l^2}\frac{\sin\left(\Delta G_y m\frac{b}{2}\right)}{\Delta G_y b}\quad \text{for } \Delta G_x=0,\ \Delta G_y\neq 0,$$

$$-V_0\frac{2m}{l^2}\frac{\sin\left(\Delta G_x m\frac{b}{2}\right)}{\Delta G_x b}\quad \text{for } \Delta G_x\neq 0,\ \Delta G_y=0, \quad (7)$$

$$-\frac{V_0}{l^2}\frac{\sin\left(\Delta G_x m\frac{b}{2}\right)}{\Delta G_x b}\frac{\sin\left(\Delta G_y m\frac{b}{2}\right)}{\Delta G_y b}\quad \text{for } \Delta G_x\neq 0,\ \Delta G_y\neq 0,$$

where $\mathbf{G}$ is the reciprocal-lattice vector of the bulk, $b=(\sqrt{2}/2)a$, and mb is the width of the wire ($m<l$), $\Delta\mathbf{G}=\mathbf{g}+\mathbf{G}-\mathbf{g}'-\mathbf{G}'$.

The form factors of the empirical pseudopotentials $V_s(3)$, $V_s(8)$, $V_s(11)$, and $V_A(3)$, $V_A(4)$, and $V_A(11)$ are not enough for the double-unit-cell energy-band calculation, so we fit the atomic form factors by an analytical formula. The atomic form factors for the empirical pseudopotential used in this paper are listed in Table I

The optical transition matrix elements and corresponding lifetime are given by

$$Q^i_{nn'}=\frac{1}{m_0}|\langle n|p_i|n'\rangle|^2,\quad i=x,y,z, \quad (8)$$

and[9]

TABLE I. Fitted form factors $V(2\pi\sqrt{N}/a)$ of the atomic empirical pseudopotential normalized to the atomic volume (in units of Ry). a is the lattice constant.

	Si	Ga	As	Zn	Se
a (Å)	5.43	5.64	5.64	5.65	5.65
$N=1$	−0.3622	−0.3075	−0.5082	−0.1055	−0.6799
2	−0.2779	−0.2377	−0.3948	−0.0797	−0.5320
3	−0.2100	−0.1816	−0.2999	−0.0500	−0.4104
4	−0.1510	−0.1328	−0.2200	−0.0190	−0.3105
5	−0.0978	−0.0888	−0.1522	0.0110	−0.2284
6	−0.0488	−0.0483	−0.0947	0.0381	−0.1609
7	−0.0031	−0.0105	−0.0458	0.0610	−0.1055
8	0.0394	0.0252	−0.0049	0.0789	−0.0599
9	0.0761	0.0586	0.0271	0.0913	−0.0224
10	0.0955	0.0871	0.0466	0.0971	0.0080
11	0.0800	0.0946	0.0500	0.0900	0.0304
12	0.0436	0.0640	0.0400	0.0555	0.0391

$$\frac{l}{\tau}=\frac{4\alpha\omega n}{3m_0c^2}Q_{nn'}, \tag{9}$$

where α is the fine structure constant, ω is the photon angular frequency, and n is the refractive index.

III. RESULTS OF Si WIRES

In all calculations in this paper we take $l=7$, $m=5$, 4, 3, and 2, and the four lowest conduction-band states and four highest valence-band states of the bulk as basis functions in Eq. (5), hence we have only 196 basis functions in the wave-function expansion. The V_0 values are taken as 8 and −6 eV for the conduction and valence-band states, respectively.

The eigenenergies of the lowest four conduction-band states and the highest four valence-band states at the Γ point for $m=5$, 4, 3, and 2 structures are shown in Table II, and the energy gap as function of the wire width is shown in Fig. 1. From Table II we see that the electronic ground state ($C1$) is singlefold, and the second and third excited states ($C2$ and $C3$) are twofold degenerate. The two highest states of the hole ($V1$ and $V2$) are twofold degenerate. Figure 2 compares our calculated energy gaps with other theoretical results for the Si wire case. From Fig. 2 we see that for the number of monolayers, $N=8$ and 10, our results are in agreement with the results of Ref. 9, which also used the empirical pseudopotential method. But for the cases when $N=6$ and 4, our calculated energy gaps are larger than those of Ref. 9. This is because as the wire becomes thinner, the proportion of surface atoms relative to the atoms in the bulk becomes larger. Then surface states will dominate the energy gap of the wire. In our calculation we use an ideal potential barrier to deal with the surface [cf. Eq. (7)]. Hence, our results represent the energy gaps caused by quantum confinement effect only, while the results of Ref. 9 depend on the surface state (with or without H covered as in Ref. 9), especially in the case of a thin wire. The other three results Read *et al.*,[10] Buda, Kahanolf, and Parrinello,[11] and Ohno, Shiraishi, and Ogawa[12] are based on the first-principles pseudopotential calculation with the local-density approximation (LDA) for the exchange-correlation energy and potential. From Fig. 2, we see that these three groups of energy gaps are all smaller than energy gaps calculated with the empirical pseudopotential method. The first-principles pseudopotential method with the LDA can predict with good accuracy the properties of ground states, such as total energy, force constants, construction phase transition etc., but cannot give an accurate behavior of the excited states. For example, it consistently underestimates the energy gap. On the other hand, the empirical pseudopotential method, though empirical and simple, can produce accurate conduction and valence states, therefore it is more suitable for studying the quantum confinement effect of a quantum wire.

The wave functions of the electronic states consist of mainly four bulk Δ states in the x-y plane, the components of states near the Γ point increase with a decreasing width of the wire (m). Using Eq. (8) we calculated the optical transition matrix elements for $C1$, $C2$ states to $V1$, $V2$ states. The results are shown in Table III, where the first number represents that for polarization along the x and y directions (average), and the second number is for polarization along the z direction (wire direction). From Table III we see that the

TABLE II. Energy levels of quantum wires relative to the valence-band top (in units of eV). m represents the width of the wire (see text), Cn and Vn are the conduction- and valence-band states, respectively.

		$C1$	$C2$	$C3$	$C4$	$V1$	$V2$	$V3$	$V4$
Si	$m=5$	1.314	1.334	1.334	1.342	−0.550	−0.551	−0.595	−0.607
	4	1.570	1.593	1.593	1.594	−0.825	−0.825	−0.862	−0.925
	3	2.062	2.073	2.087	2.092	−1.239	−1.240	−1.339	−1.488
	2	3.376	3.411	3.418	3.435	−2.203	−2.205	−2.254	−2.724
GaAs	$m=5$	2.352	2.353	2.507	2.537	−0.360	−0.437	−0.545	−0.545
	4	2.569	2.569	2.796	2.853	−0.534	−0.650	−0.813	−0.813
	3	3.004	3.005	3.270	3.414	−0.867	−1.044	−1.281	−1.281
	2	4.328	4.339	4.734	4.899	−1.573	−1.886	−2.194	−2.195
ZnSe	$m=5$	3.565	4.383	4.383	4.969	−0.152	−0.189	−0.263	−0.264
	4	3.910	4.890	4.890	5.196	−0.232	−0.292	−0.394	−0.396
	3	4.501	5.478	5.478	5.646	−0.402	−0.494	−0.641	−0.643
	2	5.781	6.634	6.635	6.643	−0.793	−0.998	−1.338	−1.341

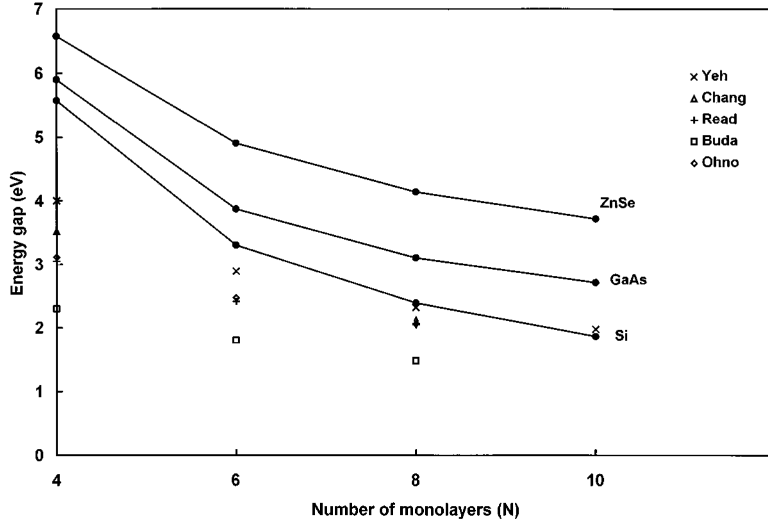

FIG. 2. Energy gaps of three semiconductors wires as functions of the number of monolayers for each edge. The present results are indicated by filled circles connected by lines. The discrete points are theoretical energy gaps of Si wires taken from Refs. 9 (Yeh), 7 (Chang), 10 (Read), 11 (Buda), and 12 (Ohno), respectively.

optical transition matrix elements are small compared to the direct transition in bulk GaAs (about several eV), which means that the energy gap is pseudodirect, as shown by the wave-function composition. When the width of wire m decreases from 5 to 3 (19.2 Å to 11.5 Å) the optical transition matrix elements increase due to the mixing of the bulk Δ states and near-Γ states. At $m=2$ (7.7 Å) there is an abrupt change, and the optical transition matrix elements for the z polarization reach 1.7 eV, as in the direct transition. This is caused by the mixing of the bulk Δ and Γ_{15} states. At $m=5$, 4, and 3, the wave function of the $C1$ state does not consist of Γ_{15} state components, but at $m=2$ it consists of Γ_{15} state components, resulting in a direct transition. Because the effective mass of the Γ_{15} state is large (even negative), as the width of wire decreases due to the quantum confinement the Δ states approaches the Γ_{15} state, there occurs a strong mixing of these two states. This result is consistent with Sanders and Chang's result of the tight-binding calculation for thin Si wires.[7]

We compare our theoretical results with the room-temperature time-resolved PL experiment.[13] The main emission peaks and lifetimes observed by Calcott *et al.* are schematically shown in Fig. 3. The wire width has a broad distribution 30±10 Å as in Ref. 11, so we take our $m=5$ (19.2 Å) results. From Tables II and III we see that the lowest transitions are $C1-V1$ $(V2)$ and $C2-V1$ $(V2)$ (because $V1$ and $V2$ are degenerate), and the optical transition energies are 1.86 and 1.88 eV, respectively, with an energy difference of 20 meV. The corresponding optical transition matrix elements $Q_{nn'}$ [Eq. (8)] are 9.41×10^{-7} and 1.34×10^{-3} eV, respectively. Inserting the $Q_{nn'}$'s into Eq. (9), we obtain the lifetimes 2.1 ms and 1.5 μs, in good agreement with the experiment. This result verifies that there surely exist optical transitions between quantum confinement states in porous silicon, though the luminescence strength is not large enough to explain the strong luminescence.

The calculated lifetimes as functions of the number of monolayers, N, together with the results of Ref 9, are shown in Fig. 4. From Fig. 4, we see that, as N decreases, the lifetimes for CS1 and CS2 states decrease, and cross near $N=6$. They have the minimum values of 3.9×10^{-10} and 3×10^{-9} s on $N=4$, which are characteristics of direct transi-

TABLE III. Optical transition matrix elements (in units of eV) for $C1$ and $C2$ states to $V1$ and $V2$ states. The first number is for the x,y polarization (average), the second number is for the z polarization, m is the width of wire, and values less than 1–10 are set to zero.

		$C1$-$V1$		$C1$-$V2$		$C2$-$V1$		$C2$-$V2$	
Si	$m=5$	9.41−7	2.29−9	9.01−7	0	1.47−6	1.34−3	1.46−6	2.54−4
	4	4.13−5	0	4.11−5	4.86−7	5.93−6	2.61−2	6.50−6	4.96−3
	3	2.07−3	0	2.09−3	0	4.00−3	0	4.05−3	1.66−6
	2	4.14−4	1.73	4.06−4	2.18−1	8.64−4	1.85−1	8.56−4	1.49
GaAs	$m=5$	1.82−4	0	1.21−6	0	7.00−5	0	1.41−6	0
	4	3.24−3	0	2.70−3	0	2.65−3	0	2.71−3	0
	3	5.87−2	0	1.24−1	0	5.40−2	0	1.24−1	0
	2	3.89−1	0	6.40−1	0	3.57−1	0	6.46−1	0
ZnSe	$m=5$	0	5.34	0	0	1.43−3	0	1.44	0
	4	0	5.05	0	0	3.83−3	0	1.42	0
	3	0	4.67	0	0	1.22−2	0	8.09−1	0
	2	0	4.07	0	0	7.81−2	0	8.17−1	0

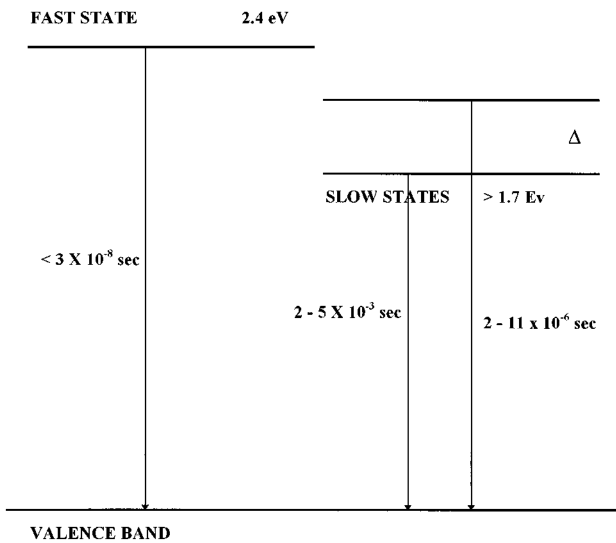

FIG. 3. Schematic depiction of the main emission peaks and lifetimes observed by Calcott *et al.* (Ref. 13) for anodically prepared porous Si. The figure is taken from Ref. 9.

tion, whereas Ref. 9 shows that the two lifetimes of CS1 and CS2 states decrease monotonously with decreasing N until $N=6$, but with no result on $N=4$. As mentioned above, this contradiction may be due to the surface state effect for thin wires.

IV. RESULTS OF GaAs AND ZnSe WIRES

Our model can be applied equally to other semiconductor wires, because the model does not add any restricted condition to the boundary, only a constant potential barrier. The eigenenergies of the conduction- and valence-band states for GaAs and ZnSe wires are shown in Table II, the energy gaps as functions of the width of wire are shown in Fig. 2, and the optical transition matrix elements are shown in Table III. From Table II we see that for a GaAs wire the first two electronic states ($C1$ and $C2$) are twofold degenerate, and the third and fourth hole states ($V3$ and $V4$) are twofold degenerate. For a ZnSe wire the second and third electronic states ($C2$ and $C3$) are twofold degenerate, and the third and fourth hole states ($V3$ and $V4$) are twofold degenerate. The degenerate states are different for these three kinds of wire. From Table III we see that the GaAs wire becomes an indirect gap semiconductor just like the Si wire. This is a surprising result. From the wave functions of the conduction-band states $C1$ and $C2$ we see that they consist of mainly four bulk Δ states, resulting in an indirect transition. At the Γ point of the Brillouin zone of bulk GaAs, the lowest conduction-band state is the Γ_1 state, from which the transition to valence-band top states is the direct transition. But the effective mass of the Γ_1 state is small compared to that of the Δ states in the axial direction. When the width of the wire decreases, the Γ_1 state rises faster than the Δ states, at a critical width there occurs a Γ-Δ crossover, the Γ_1 state becomes higher than Δ states, and the GaAs wire changes from a direct energy gap to an indirect energy gap. This case is something like the Γ-X crossover in the GaAs AlAs short-period superlattices.[15–19] When the period of the GaAs/AlAs superlattice decreases, the X state confined in the AlAs quantum well becomes lower than the Γ state confined in the GaAs quantum well, and the superlattice changes from a direct energy gap to an indirect energy gap. In the case of the superlattice the X state is provided by AlAs, while in the case of wire the Δ states are provided by GaAs. Because the effective mass of the Γ_1 state is small, until the width of wire m decreases to 2 (7.7 Å) the wave functions of the lowest conduction-band states ($C1$ and $C2$) do not consist of the component of bulk Γ_1 state, hence the GaAs wire is still an indirect energy gap semiconductor. But from Table III we see that the optical transition matrix elements of the GaAs wire are larger than those of the Si wire by about two orders of magnitude for the same width, and increase with decreasing width.

The ZnSe wire shows another characteristics. From Table III we see that the ZnSe wire is always a direct energy gap semiconductor until the width of wire m decreases to 2. Because the bulk Δ states are far higher than the bulk Γ_1 state by 1.7 eV, furthermore the effective mass of the ZnSe Γ_1 state is rather large ($0.15m_0$), hence the bulk Γ_1 state is always lower than the bulk Δ states as the width of wire decreases to 2. The wave function of the electronic ground state ($C1$) includes the large component of the bulk Γ_1 state 0.42 and 0.12 for wire widths $m=5$ and 2, respectively. From Table III we see that the direct transition matrix elements for the electronic ground state are not equal to zero only for the z polarization, which is verified by the experiments[20,21] and the effective-mass theory.[21] The direct optical transition matrix elements decrease, with the width of the wire decreasing due to the mixing of the bulk Γ_1 state and other states. Experimentally it is found that a II-VI compound semiconductor cluster of 20–200 Å shows good luminescence characters;[22] our results prove theoretically that the optical transition is direct in these thin quantum wires or dots, and give a fine prospect for them in the practical application.

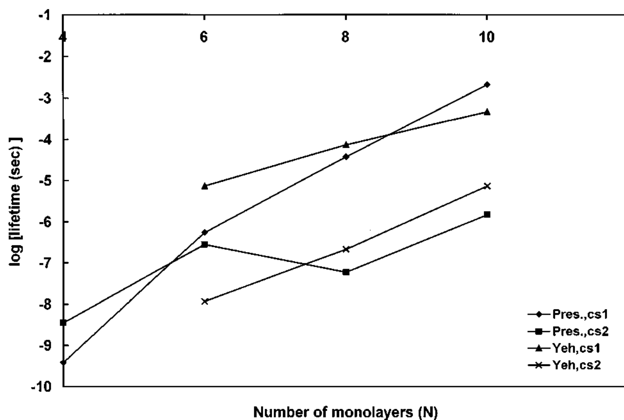

FIG. 4. Calculated radiative lifetimes for the lowest two conduction states (CS1 and CS2) to the highest valence states as functions of the number of monolayer for each edge. The two groups are present results and those of Ref. 9.

V. SUMMARY

In this paper we studied the electronic states and optical transition properties of three semiconductor wires Si, GaAs,

and ZnSe, using the empirical pseudopotential homojunction model. The energy levels, wave functions, optical transition matrix elements, and lifetimes are obtained for wires of square cross section with widths from 2 to 5 ($\sqrt{2}a/2$). It is found that these three kinds of wires have different quantum confinement properties. For Si wires, the energy gap is pseudodirect, and the wave function of the electronic ground state consists of mainly four bulk Δ states. The optical transition matrix elements are much smaller than those of a direct transition, and increase with the decreasing width of the wire. When the width of wire is 7.7 Å, the Si wire changes from an indirect energy gap semiconductor to a direct energy gap semiconductor due to mixing of the bulk Γ_{15} state. For GaAs wires, the energy gap is also pseudodirect in the width range considered, but the optical transition matrix elements are larger than those of Si wires by two orders of magnitude for the same width. At the smallest width there is no transfer to the direct energy gap as in the Si wire. For the ZnSe wires, the energy gap is always direct, and the optical transition matrix elements are comparable with those of direct energy gap bulk semiconductors. They decrease with decreasing wire width due to the mixing of the bulk Γ_1 state and other states. All the quantum confinement properties are discussed and explained by our theoretical model and the semiconductor energy-band structures. The calculated lifetimes of the Si wire and the positions of PL peaks are in good agreement with the experimental results of Calcott *et al.*[13] The theoretical model has some advantages compared to the direct pseudopotential calculation. If we perform the direct pseudopotential calculation we need to use 6000 plane waves. The secular equation cannot be solved without using a sophisticated computer, while the dimension of the secular equation in our model is only 196. The wave functions calculated by our model obviously consist of components of bulk states in the Brillouin zone, so it is convenient to analyze the transition property. Our model does not put any restricted condition on the boundary, hence it can be applied to any semiconductor wires, and takes into account the pure quantum confinement effect.[21,22]

ACKNOWLEDGMENT

This work was supported by a Croucher Foundation Research Grant.

*Permanent address: Institute of Semiconductor, Chinese Academy of Sciences, P.O. Box 912, 100083 Beijing, People's Republic of China.

†To whom all correspondence should be addressed. Electronic address: kwcheah@hkbu.edu.hk

[1] L. T. Chanham, Appl. Phys. Lett. **57**, 1046 (1990).

[2] A. C. Cullis and L. T. Canham, Nature **353**, 335 (1991).

[3] P. Deak, M. Rosenbauer, M. Stutzmann, J. Weber, and M. S. Brandt, Phys. Rev. Lett. **69**, 2531 (1991).

[4] M. S. Brandt, H. D. Fuchs, M. Stutzmann, J. Weber, and M. Cardona, Solid State Commun. **81**, 307 (1992).

[5] Y. H. Xie, W. L. Wilson, F. M. Ross, J. A. Mucha, E. A. Fitzgerald, J. M. Macaulay, and T. D. Harris, J. Appl. Phys. **71**, 2403 (1992).

[6] V. Petrova-Koch, T. Muschik, A. Kux, B. K. Meyer, F. Koch, and V. Lehmann, Appl. Phys. Lett. **61**, 943 (1992).

[7] G. D. Sanders and Y. C. Chang, Phys. Rev. B **45**, 9202 (1992).

[8] J. B. Xia and Y. C. Chang, Phys. Rev. B. **48**, 5179 (1993).

[9] C. Y. Yeh, S. B. Zhang, and A. Zunger, Phys. Rev. B **50**, 14 405 (1994).

[10] A. J. Read, R. J. Needs, K. J. Nash, L. T. Canham, P. D. J. Calcott, and A. Qteish, Phys. Rev. Lett. **69**, 1232 (1992).

[11] F. Buda, J. Kohanoff, and M. Parrinello, Phys. Rev. Lett. **69**, 1272 (1992).

[12] T. Ohno, K. Shiraishi, and T. Ogawa, Phys. Rev. Lett. **69**, 2400 (1992).

[13] P. D. J. Calcott, K. J. Nash, L. T. Canham, M. J. Kane, and D. Brumhead, J. Phys. C **5**, L91 (1993).

[14] Y. H. Xie, M. S. Hybertsen, W. L. Wilson, S. A. Ipri, G. E. Carver, W. L. Brown, E. Dons, B. E. Weir, A. R. Kortan, G. P. Watson, and A. J. Liddle, Phys. Rev. B **49**, 5386 (1994).

[15] J. Nagle, M. Garriga, W. Stolz, T. Isu, and K. Ploog, J. Phys. (Paris) Colloq. **48**, C5-495 (1987), and K. J. Moore, P. Dawson, and C. T. Foxon, *ibid.* C5-525 (1987).

[16] M. H. Meynadier, R. E. Nahory, J. M. Worlock, M. C. Tamargo, J. L. de Miguel, and M. D. Sturge, Phys. Rev. Lett. **60**, 1338 (1988).

[17] G. H. Li, D. S. Jisng, H. X. Han, Z. P. Wang, and K. Ploog, Phys. Rev. B **40**, 6101 (1989).

[18] J. B. Xia, Phys. Rev. B **39**, 3310 (1989).

[19] J. B. Xia and Y. C. Chang, Phys. Rev. B **42**, 1781 (1990).

[20] P. Ils, Ch. Greus, A. Forchel, V. D. Kulakovskii, N. A. Gippius, and S. G. Tikhodeev, Phys. Rev. B **51**, 4272 (1995).

[21] W. H. Zheng, J. B. Xia, and K. W. Cheah (unpublished).

[22] For reviews, see L. E. Brus, J. Phys. Chem. **90**, 2555 (1986), IEEE J. Quantum Electron. **22**, 1909 (1986).